MATHEMATICAL SIMULATION OF ELECTROCHEMICAL MACHINING TAKING INTO ACCOUNT THE INFLUENCE OF ELECTRODE POLARIZATION, ELECTROLYTE TEMPERATURE AND BUBBLE FORMATION ON THE FORM OF THE WORKPIECE*

Petr Novák[a], Ivo Roušar[a], Arnošt Kimla[b], Václav Cezner[a] and Vladimír Mejta[a]

[a] *Department of Inorganic Technology and*
[b] *Department of Mathematics,*
Prague Institute of Chemical Technology, 166 28 Prague 6

Received April 9th, 1979

To study the influence of polarization on the form of the workpiece, a method of transformation of the interelectrode space to a rectangle (for a two-dimensional system) was proposed. The potentials in this region were calculated by the superrelaxation method. The results of the calculation show a pronounced effect of polarization on the final form of the workpiece in comparison with an analogous calculation involving no electrode polarization. The Joule heat evolved in the streaming electrolyte and gas bubbles formed during electrolysis have also a pronounced influence on the course of the machining process.

In proposing tools for electrochemical machining, either approximate methods[1-3] or the solution of Laplace's equation in the interelectrode space[4] are used. Owing to difficulties encountered in solving these problems, nonpolarizable electrodes are usually assumed. The present work deals with calculations for a practical case of machining to show the changes in the form of the workpiece resulting from heating of the electrolyte, bubble formation, and electrode polarization in comparison with the case where only polarization of the electrodes under isothermal conditions is considered.

Formulation of the Problem

During electrochemical machining with direct current, the form of the cathode does not change while the anode dissolves gradually and its form changes. We shall consider the two-dimensional case where the cathode is planar with a triangular projection. The simulation of machining, *i.e.*, of the gradual formation of a replica of this projection on the anode surface can be represented by the following sequence of calculations: *1*) We calculate the potential distribution in the space (surface) delimited by the cathode and anode, *i.e.*, by the curves $\alpha(x)$ and $\beta(x)$, by solving Laplace's

* Part XV in the series Flow Electrolyzers; Part XIV: This Journal *45*, 1456 (1980).

equation. *2*) We calculate the local current densities on the anode and on the cathode. *3*) We calculate the loss of the metal due to electrochemical dissolution in a point, x, during a time interval, $\Delta\tau$, using Faraday's law. We take into account the eventual oxygen evolution on the anode. From the loss of the metal, we calculate the shift of the coordinates of the curve describing the shape of the anode, and this in the direction normal to its surface. At the same time, we assume that the cathode was shifted toward the anode during the time $\Delta\tau$ by a step Δy. If $\Delta\tau$ is sufficiently small, we come close to the real course of the machining. These calculations lead to a new form of the anode surface. *4*) We express the new form of the anode surface in the form of a table of mutually corresponding coordinate pairs (x_i, y_i), $i = 1,2, \ldots, N$, where N is the number of nodal points on the anode surface. *5*) We rerurn to step *1*). If the coordinates determining the form of the anode. *i.e.* $\beta(x)$, do not change any more with time, the stationary state is attained and the calculation is stopped.

In the case of the method of finite differences with time-independent values of the coordinates in the grid points, we should examine the position of the points on the boundary and the distances of the individual points from the actual interface. Since this method of calculating the potentials on the contour of the anode and the programming would be very complicated, it is preferable to use more complex relations for the calculation of the potential values in the interelectrode space, but to preserve the simple relations for the calculation of the potential values on the boundary regardless of the changes of its form. These conditions can be fulfilled by using a transformation of the space region delimited by the curves $y = \beta(x)$ and $y = \alpha(x)$ to a rectangle.

Transformation of the Interelectrode Region to a Rectangle

Since the properties of the system do not change along the z axis, the sought potential φ is described by the partial differential equation

$$\frac{\partial^2\varphi}{\partial x^2} + \frac{\partial^2\varphi}{\partial y^2} - \frac{1}{\varrho_{M(x)}} \frac{d\varrho_{M(x)}}{dx} \frac{\partial\varphi}{\partial x} = 0 . \qquad (1)$$

The derivation of this equation is given in the Appendix. It is to be solved in the region delimited by the curves

$$x = a, \quad x = b, \quad y = \alpha(x), \quad y = \beta(x) .$$

The transformation is illustrated in Fig. 1. We shall introduce the following curvilinear coordinates:

$$\xi = x, \quad \eta = (y - \alpha(x))/(\beta(x) - \alpha(x)) , \qquad (2), (3)$$

where $\xi \in \langle a; b\rangle$, $\eta \in \langle 0; 1\rangle$. The the potential $\varphi(x, y)$ is transformed to $\psi(\xi, \eta)$ and the Laplace's equation is transformed into the form

$$\frac{\partial^2\psi}{\partial\xi^2} + \frac{\partial^2\psi}{\partial\eta^2} F_1(\xi, \eta) - \frac{\partial^2\psi}{\partial\xi\,\partial\eta} F_2(\xi, \eta) - \frac{\partial\psi}{\partial\eta} F_3(\xi, \eta) - \frac{\partial\psi}{\partial\xi} G(\xi) = 0\,, \qquad (4)$$

where

$$F_1(\xi, \eta) = [\beta(\xi) - \alpha(\xi)]^{-2} [1 + (\alpha'(\xi)(1 - \eta) + \beta'(\xi)\eta)^2] \qquad (5)$$

$$F_2(\xi, \eta) = 2[\beta(\xi) - \alpha(\xi)]^{-1} [\alpha'(\xi)(1 - \eta) + \beta'(\xi)\eta] \qquad (6)$$

$$F_3(\xi, \eta) = [\beta(\xi) - \alpha(\xi)]^{-2} [(\beta(\xi) - \alpha(\xi))(1 - \eta)\alpha''(\xi) + (\beta(\xi) - \alpha(\xi))\eta\beta''(\xi) - 2(\beta'(\xi) - \alpha'(\xi)) \,.\, (\alpha'(\xi)(1 - \eta) + \beta'(\xi)\eta)] \,. \qquad (7)$$

$$G(\xi) = \frac{1}{\varrho_M(\xi)} \frac{\mathrm{d}\varrho_M(\xi)}{\mathrm{d}\xi}, \quad \alpha'(\xi) = \frac{\mathrm{d}\alpha(\xi)}{\mathrm{d}\xi} \qquad (8), (9)$$

$$\alpha''(\xi) = \frac{\mathrm{d}^2\alpha(\xi)}{\mathrm{d}\xi^2}, \quad \beta'(\xi) = \frac{\mathrm{d}\beta(\xi)}{\mathrm{d}\xi}, \quad \beta''(\xi) = \frac{\mathrm{d}^2\beta(\xi)}{\mathrm{d}\xi^2}. \quad (10), (11), (12)$$

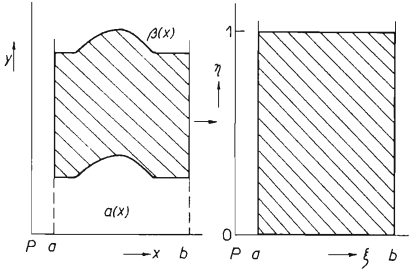

FIG. 1
Transformation of the Region Delimited by Curves $\alpha(x)$ and $\beta(x)$ to a Rectangle

The boundary conditions for Eq. (*4*) are:

$$\xi = a \quad \text{or} \quad \xi = b : \quad \partial\psi/\partial\xi = 0 , \tag{13}$$

i.e., the planes $\xi = a$ and $\xi = b$ are symmetrical, or no current flows out from the space between the electrodes.

The potential in the electrolyte at the anode or cathode surface can be determined from the definition of the electrode potential:

$$E_A = \varphi_{m,A} - \varphi_{s,A} + \text{const.} , \quad E_K = \varphi_{m,K} - \varphi_{s,K} + \text{const.} \tag{14), (15}$$

Since the constants are related to the choice of the reference electrode, they can be set equal to zero. For the same reason, we can set $\varphi_{m,K} = 0$, but then $\varphi_{m,A}$ is equal to the terminal voltage, U, of the electrolyser. Then

$$\psi_A = U - E_A(i_{n,A}) , \quad \psi_K = -E_K(i_{n,K}) , \tag{16), (17}$$

where $U > 0$. The dependence of the electrode potentials E_A and E_K on the current density i is given by the Tafel equation; hence

$$\psi_A = U - E_{r,A} - a_A - b_A \ln i_{n,A} , \tag{18}$$

$$\psi_K = -E_{r,K} + a_K + b_K \ln |i_{n,K}| . \tag{19}$$

These expressions are simplified in the region close to the equilibrium potential $E_{r,A}$ or $E_{r,K}$ as follows:

$$\psi_A = U - E_{r,A} - i_{n,A}/k_A , \quad \psi_K = -E_{r,K} + |i_{n,K}|/k_K . \tag{20), (21}$$

The linearized expressions (*20*) and (*21*) are used for low current densities defined as

$$i_{n,A} < \exp [(b_A - a_A)/b_A] , \quad |i_{n,K}| < \exp [(b_K - a_K)/b_K] . \tag{22), (23}$$

Eqs (*18*) and (*19*) serve for higher current densities. The constants k_A and k_K are given as

$$k_A = b_A^{-1} \exp [(b_A - a_A)/b_A] , \quad k_K = b_K^{-1} \exp [(b_K - a_K)/b_K] . \tag{24), (25}$$

The current densities at the surface of the anode ($\beta(x)$) and cathode ($\alpha(x)$) are given as

$$|i_n| = \varrho_M^{-1} |(\text{grad } \varphi)_n| , \tag{26}$$

where the potential gradient for the cathode is

$$(\text{grad } \varphi)_{n,K} = (1 + \alpha'^2)^{-1/2} \left[\left(\frac{\partial \psi}{\partial \eta} \right)_\alpha \frac{1 + \alpha'^2}{\beta - \alpha} - \left(\frac{\partial \psi}{\partial \xi} \right)_\alpha \alpha' \right] \tag{27}$$

and for the anode

$$(\text{grad } \varphi)_{n,A} = (1 + \beta'^2)^{-1/2} \left[\left(\frac{\partial \psi}{\partial \eta} \right)_\beta \frac{1 + \beta'^2}{\beta - \alpha} - \left(\frac{\partial \psi}{\partial \xi} \right)_\beta \beta' \right]. \tag{28}$$

Since the anodic current density is considered positive and the cathodic one negative, the normal components of the gradients must be provided with the corresponding sign, which depends on the choice of the normal direction.

The specific resistance ϱ_M of the bubble-electrolyte mixture is given by the equation

$$\varrho_M(x) = \varrho_E(x) \left[1 + 1{\cdot}5 \dot{V}_G(x) / \dot{V}_E \right], \tag{29}$$

where the volume flow of the gaseous phase is given as

$$\frac{\dot{V}_G(x)}{w} = \int_a^x \left(i_{n,K}(x) \frac{p_{G,K}}{n_{G,K}} + i_{n,A}(x) \frac{p_{G,A}}{n_{G,A}} \right) \frac{RT(x)}{FP(x)} \left[1 + (\gamma'(x))^2 \right]^{1/2} \mathrm{d}x . \tag{30}$$

We shall consider the flow of electrolyte in the direction of the x axis and we shall assume that the heat transfer into the bubble during its passage through the system is negligible. The flow line $\gamma(x)$ is defined as

$$\gamma(x) = \tfrac{1}{2}(\alpha(x) + \beta(x)) . \tag{31}$$

The dependence of the specific resistance ϱ_E on the temperature can be expressed as

$$\varrho_E = \varrho_E^0 [1 + \delta_1(T - T_0) + \delta_2(T - T_0)^2 + \delta_3(T - T_0)^3] . \tag{32}$$

The temperature in any point of the system is determined by the energy balance:

$$T(x) = T_0 + \frac{w}{\dot{V}_E S_E C_{pE}} \int_a^x \{ \varrho_M(x)\, i_{A,K}^2(x) (\beta(x) - \alpha(x)) - \left[1 + (\beta'(x))^2 \right]^{1/2} \cdot$$

$$\cdot\, k_T(x) (T(x) - T_A) - k_{T(x)} (T(x) - T_K) \left[1 + (\alpha'(x))^2 \right]^{1/2} \} \, \mathrm{d}x . \tag{33}$$

Here we neglect the enthalpy change due to electrode reactions. The mean current density $\bar{i}_{A,K}$ is defined as

$$\bar{i}_{A,K} = \tfrac{1}{2}(i_{n,A} + |i_{n,K}|) . \tag{34}$$

From Eqs (29)–(34) we obtain

$$\frac{\mathrm{d}\varrho_M(x)}{\mathrm{d}x} = w\,\varrho_E(x)\,\frac{1{\cdot}5}{\dot{V}_E}\left(i_{n,K}(x)\,\frac{p_{G,K}}{n_{G,K}} + i_{n,A}(x)\,\frac{p_{G,A}}{n_{G,A}}\right)\frac{RT(x)}{FP(x)}\,.$$

$$.\,[1 + (\gamma'(x))^2]^{1/2} + \frac{w}{\dot{V}_E S_E C_{pE}}\left(1 + 1{\cdot}5\,\frac{\dot{V}_G(x)}{\dot{V}_E}\right)\varrho_E^0[\delta_1 + 2\delta_2(T(x) - T_0) +$$

$$+ 3\delta_3(T(x) - T_0)^2]\,[\varrho_M(x)\,i_{A,K}^2(x)\,(\beta(x) - \alpha(x)) - k_T(x)\,(T(x) - T_A)\,.$$

$$.\,[1 + (\beta'(x))^2]^{1/2} - k_T(x)\,(T(x) - T_K)\,[1 + (\alpha'(x))^2]^{1/2}\,. \qquad (35)$$

(The primes denote differentiation with respect to x.) The heat transfer is calculated with the use of equations valid for a fully developed turbulent profile, so that in our case, where the cross section changes along the flow line, the values are subject to some error.

The coefficient of heat transfer k_T is calculated from the definition of the Nusselt's criterion:

$$\mathrm{Nu}(x) = k_T(x)\,\mathrm{d}_e(x)/\lambda\,. \qquad (36)$$

The equivalent diameter d_e is defined as

$$d_e = 2A/w\,, \qquad (37)$$

where the cross-sectional area of flow, A, is approximated as

$$A = w(\beta(x) - \alpha(x))/[1 + (\gamma'(x))^2]^{1/2}\,. \qquad (38)$$

The Nusselt's criterion is given by the equation

$$\mathrm{Nu}(x) = 0{\cdot}023\,\mathrm{Re}^{0.8}(x)\,\mathrm{Pr}^{0.4}(x)\,, \qquad (39)$$

where

$$\mathrm{Re}(x) = 2\dot{V}_E S_E/w\,\mu(x)\,, \quad \mathrm{Pr}(x) = C_p\,\mu(x)/\lambda\,. \qquad (40), (41)$$

Eq. (39) holds in the turbulent region, but is can be used in the case of a channel of changing form as a first approximation if the Reynolds number is larger than 1000. The dependence of the viscosity on the temperature is given by the approximate equation[5]

$$\varrho_E(x)/\mu(x) = \text{const.} \qquad (42)$$

The density of the electrolyte, S_E, its specific heat capacity, C_{pE}, and thermal conductivity will be considered constant. The pressure as a funxtion of x is calculated from the equation

$$P(x) = P^0 - \int_a^x \frac{0{\cdot}3164 S_E (1 - f(x))}{\mathrm{Re}_M^{1/4}(x)\,(\beta(x) - \alpha(x))} \left(\frac{\dot{V}_E}{w(\beta(x) - \alpha(x))} \right)^2 \frac{[1 + (\gamma'(x))^2]^{1/2}}{2(1 - f(x))^2}\, \mathrm{d}x\,, \tag{43}$$

where[6]

$$\mathrm{Re}_M(x) = \mathrm{Re}(x)\,(1 - \mathrm{f}(x))^{2{\cdot}5}\,, \quad \mathrm{f}(x) = \dot{V}_G(x)/(\dot{V}_E + \dot{V}_G(x))\,. \tag{44), (45}$$

Since it is not possible to express the temperature and pressure explicitly from the above equations, we proceed by iteration so that we calculate alternately the pressure and the temperature using the equations

$$P^{S+1}(x) = C_1\, P^N(x) + (1 - C_1)\, P^S(x)\,, \tag{46}$$

$$T^{S+1}(x) = C_2\, T^N(x) + (1 - C_2)\, T^S(x)\,, \tag{47}$$

where $C_1, C_2 \in \langle 0{\cdot}1; 0{\cdot}3 \rangle$.

If we solve the Laplace's equation in the region corresponding to the interelectrode space, we must correct the potentials at the boundaries in order that they correspond to Eqs (*18*)–(*21*). We therefore calculate the local current densities from Eq. (*26*) and iterate in turn the potentials ψ_A and ψ_K until Eqs (*18*)–(*21*) and (*26*) are fulfilled. A preferred iteration procedure uses, *e.g.*, for the anode the relation

$$\psi_A^{S+1} = C_3\, \psi_A^N + (1 - C_3)\, \psi_A^S\,, \tag{48}$$

where $C_3 \in \langle 0{\cdot}001; 0{\cdot}05 \rangle$, ψ_A^S is the past value of the potential, and ψ_A^N is the potential value calculated by substituting the corresponding current density into Eqs (*18*)–(*21*). To speed up the convergence, we correct the local current densities in the following way: we calculate the total currents for the anode and cathode

$$I_A = \int_a^b i_{N,A}[1 + (\beta')^2]\, \mathrm{d}x\,, \tag{49}$$

$$I_K = \int_a^b i_{N,K}[1 + (\alpha')^2]\, \mathrm{d}x\,. \tag{50}$$

Now we define

$$I_S = \tfrac{1}{2}(I_A + I_K) \tag{51}$$

and we multiply the current densities calculated from Eq. (*26*) by the ratio I_S/I_A or I_S/I_K. These corrections are unimportant at the end of the calculation, when $I_A = I_K$.

To ensure the convergence of the potentials in the interelectrode region, we take only a certain fraction of the newly calculated potentials ψ_A and ψ_K:

$$\psi_A^{q+1} = C_4 \psi_A^N + (1 - C_4) \psi_A^q , \tag{52}$$

where $C_4 \in \langle 0{\cdot}4; 1{\cdot}0 \rangle$ and ψ_A^q is the anode potential from the past calculation. The calculation of the potentials on the boundaries is carried out after 5–20 iterations within the field. Similarly the new values of the specific resistance are calculated from Eq. (*29*) after 5–20 iterations within the field. A direct calculation of the potentials on the boundary from Eqs (*20*) and (*21*) is possible in the region of low current densities, however even here we prefer the iterative calculation since the algorithm of the computational procedure becomes simpler.

After attaining the required accuracy of the potentials (both in the field and on the boundaries), temperatures and pressures, we consider a change of the form of the anode. We assume that the current densities on the electrode surface do not change during a small time interval $\Delta\tau$, so that it is possible to calculate the shift rate of the anode in the direction of the normal, Δn, as

$$\Delta n = i_{n,A} M_A p_1 / n F S_A , \tag{53}$$

where p_1 denotes current yield for the anodic metal dissolution according to the reaction

$$\mathrm{Me} = \mathrm{Me}^{n+} + ne . \tag{54}$$

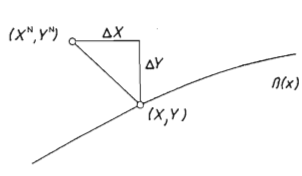

FIG. 2

Shift of Coordinates of a Point (X, Y) on the Anode Surface $\beta(x)$ During a Time $\Delta\tau$ into a Point (X^N, Y^N)

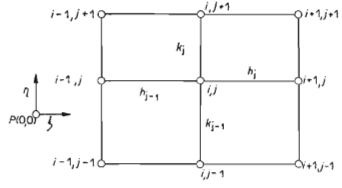

FIG. 3

Grid of Points and their Notation

If we denote the coordinates of a point on the anode surface as X, Y, where $Y = \beta(x)$, then the coordinates X^N, Y^N after the anodic dissolution for a time interval $\Delta\tau$ will be (Fig. 2)

$$X^N = X - \Delta X\,, \quad Y^N = Y + \Delta Y\,, \qquad (55), (56)$$

where

$$\Delta X = \Delta n\,\beta'\left[1 + (\beta')^2\right]^{-1/2}\Delta\tau\,, \qquad (57)$$

$$\Delta Y = \left(\Delta n\left[1 + (\beta')^2\right]^{-1/2} - v_y\right)\Delta\tau\,. \qquad (58)$$

In the latter equation we assume that the anode moves at a velocity v_y against the cathode, which is fixed.

By performing the calculation for all points on the curve $\beta(x)$, we obtain the values of $\beta^N(X^N)$, which must be recalculated for the original X values corresponding to the nodal points. This was done by quadratic interpolation.

The values of $\Delta\tau$ must be relatively small to make the changes in the electrode shape also small; thus the error of the calculation is maintained small. The described method of calculation of new values of $\beta(x)$ corresponds to the Euler's integration method. By choosing a large velocity of the electrode shift v_y we can simulate the situation when the electrodes come into contact similarly as in practice.

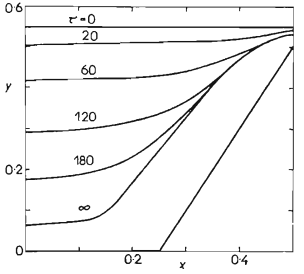

FIG. 4

Graphical Representation of Machining without Regard to Polarization, Temperature and Bubble Effects

Time τ in s.

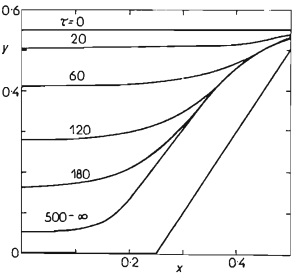

FIG. 5

Graphical Representation of Machining with Regard to the Polarization but not to the Temperature and Bubble Effects

Time τ in s.

Approximation of the Derivatives by Difference Formulas

We shall consider a two-dimensional grid with an unequal spacing (Fig. 3), in which it is possible to approximate the derivatives by difference formulas with an error of $0(h^2)$ or $0(k^2)$:

$$\left(\frac{\partial f}{\partial \xi}\right)_{i,j} = \frac{f_{(i+1)}h_{(i-1)}^2 + f_{(i)}(h_{(i)}^2 - h_{(i-1)}^2) - f_{(i-1)}h_{(i)}^2}{h_{(i)}h_{(i-1)}(h_{(i)} + h_{(i-1)})}, \tag{59}$$

$$\left(\frac{\partial^2 f}{\partial \xi^2}\right)_{i,j} = \frac{f_{(i+1)}h_{(i-1)} - f_{(i)}(h_{(i)} + h_{(i-1)}) + f_{(i-1)}h_{(i)}}{0{\cdot}5h_{(i-1)}h_{(i)}(h_{(i-1)} + h_{(i)})} \tag{60}$$

$$\left(\frac{\partial^2 f}{\partial \xi\, \partial \eta}\right)_{i,j} = \frac{h_{(i)}}{h_{(i-1)}(h_{(i-1)} + h_{(i)})}\left[\frac{f_{(i-1,j-1)}k_{(j)}}{k_{(j-1)}(k_{(j)} + k_{(j-1)})} - f_{(i-1,j)}\frac{k_{(j)} - k_{(j-1)}}{k_{(j-1)}k_{(j)}} - \right.$$

$$\left. - \frac{f_{(i-1,j+1)}k_{(j-1)}}{k_{(i)}(k_{(j-1)} + k_{(j)})}\right] + \frac{h_{(i)} - h_{(i-1)}}{h_{(i)}h_{(i-1)}}\left[-\frac{f_{(i,j-1)}k_{(j)}}{k_{(j-1)}(k_{(j-1)} + k_{(j)})} + \right.$$

$$\left. + f_{(i,j)}\frac{k_{(j)} - k_{(j-1)}}{k_{(j)}k_{(j-1)}} + \frac{f_{(i,j+1)}k_{(j-1)}}{k_{(j)}(k_{(j-1)} + k_{(j)})}\right] + \frac{h_{(i-1)}}{h_{(i)}(h_{(i-1)} + h_{(i)})} \cdot$$

$$\cdot\left[-\frac{f_{(i+1,j-1)}k_{(j)}}{k_{(j-1)}(k_{(j-1)} + k_{(j)})} + f_{(i+1,j)}\frac{k_{(j)} - k_{(j-1)}}{k_{(j)}k_{(j-1)}} + \frac{f_{(i+1,j+1)}k_{(j-1)}}{k_{(j)}(k_{(j-1)} + k_{(j)})}\right]. \tag{61}$$

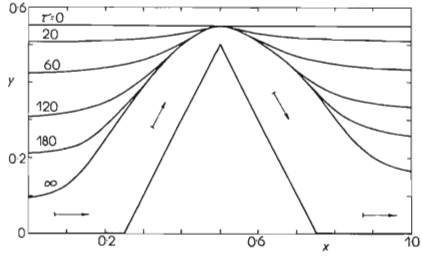

FIG. 6

Graphical Representation of Machining with Regard to the Polarization, Temperature, and Bubble Effects

Time τ in s. Electrolyte flows from left to right.

For the boundaries, asymmetrical formulas are used: if the values in the points $i + 1$ and $i + 2$ are known, we use the formula

$$\left(\frac{\partial f}{\partial \xi}\right)_i = \frac{(f_{(i+1)} - f_{(i)})\,(h_{(i)} + h_{(i+1)})^2 - (f_{(i+2)} - f_{(i)})\,h_{(i)}^2}{h_{(i)}h_{(i+1)}(h_{(i)} + h_{(i+1)})} \qquad (62)$$

and if the values in the points $i - 1$ and $i - 2$ are known, we have

$$\left(\frac{\partial f}{\partial \xi}\right)_i = \frac{(f_{(i-2)} - f_{(i)})\,h_{(i-1)}^2 - (f_{(i-1)} - f_{(i)})\,(h_{(i-2)} + h_{(i-1)})^2}{h_{(i-1)}h_{(i-2)}(h_{(i-1)} + h_{(i-2)})} \qquad (63)$$

Eqs (*62*) and (*63*) are needed in calculating the potential gradients at the electrode surface.

The iterative calculation of the potential in a given point is carried out by the relaxation method, *i.e.*, according to

$$\psi_{(i,j)}^{S+1} = \psi_{(i,j)}^{S} + r_{(i,j)}R_{(i,j)}^{S}\,. \qquad (64)$$

The superscripts S and $S + 1$ denote the iteration series. The values of $R_{(i,j)}^{S}$ are calculated by introducing the S-th potential values into the left side of Eq. (*4*) where the derivatives were replaced by the corresponding difference formulas (*59*)–(*61*).

TABLE I

Values of Constants for the Simulation of Machining

Variant	*A*	*B*	*C*
U (V)	10·000	10·000	14·114
$E_{r,A}$ (V)	1·1	1·1	1·1
$E_{r,K}$ (V)	0·0	0·0	0·0
a_A (V)	0	−0·1526	−0·1526
b_A (V)	0	0·06	0·06
a_K (V)	0	−0·0526	−0·0526
b_K (V)	0	0·06	0·06
ϱ_E^0 (10^{-2} Ωm)	2·0	2·0	2·0
p_I	1·0	1·0	1·0
$p_{G,K}$	0	0	1
$p_{G,A}$	0	0	0

The convergence of the potentials ψ^{S+1} was achieved by the following choice of the relaxation factor $r_{(i,j)}$:

$$r_{(i,j)}^{-1} = 2h^{-2} + 2\left|F_1(\xi, \eta)\right| k^{-2} + h^{-1}k^{-1}\left|F_2(\xi, \eta)\right| + k^{-1}\left|F_3(\xi, \eta)\right| + h^{-1}\left|G(\xi)\right|, \quad (65)$$

where h denotes Min (h_i, h_{i-1}) and k = Min (k_j, k_{j-1}). By this choice of the relaxation coefficient, the row norm of the coefficient matrix of the solved system of differential equations is minimized, thus ensuring convergence of the values of ψ.

RESULTS

The calculations were carried out for the case of the formation of a depression in the anode, the cathode being plate-shaped with a projection in the form of a triangle (Figs 4–6). Three variants were considered: *A*) calculation without considering polarization, electrolyte temperature and dissipated bubbles; *B*) calculation taking into account polarization, but not the temperature and bubbles; *C*) calculation taking into account all the mentioned effects.

The constants used in simulating the machining are given in Table I. The initial electrode distance was 0·55 cm, in the place of the projection only 0·05 cm. The shift

TABLE II

Profile of Anode and Current Distributions on Anode and Cathode in Stationary State for Variants *A* and *B*

x, 10^{-2} m	*A*			*B*		
	$\beta(x)$ 10^{-2} m	i_A 10^4 A/m^2	$-i_K$ 10^4 A/m^2	$\beta(x)$ 10^{-2} m	i_A 10^4 A/m^2	$-i_K$ 10^4 A/m^2
0·000	0·0633	73·4	68·7	0·0520	73·4	71·2
0·093	0·0723	68·5	60·3	0·0569	70·8	64·8
0·178	0·1299	47·4	36·1	0·1005	49·6	40·1
0·255	0·2581	37·9	18·7	0·2276	36·9	19·5
0·326	0·3747	41·7	37·1	0·3539	39·5	36·5
0·389	0·4536	49·9	41·4	0·4398	47·4	40·0
0·447	0·5057	59·8	45·2	0·4977	57·4	44·1
0·500	0·5324	73·4	294·8	0·5282	73·4	262·1[a]

[a] Peak.

rate of the anode with respect to the cathode was 0·0027 cm/s. The mean current density was 700 – 750 kA/m^2 for cases A and B and 50 – 750 kA/m^2 for case C; $\Delta\tau = 4$ s. For the case C, the temperature of both electrodes and electrolyte at the inlet was 20°C, the volume rate of flow of electrolyte referred to unit width $\dot{V}_E/w = 5 \cdot 10^{-4}$ m^2/s. The constants in Eq. (*32*) were $\delta_1 = -1{\cdot}891 \cdot 10^{-2}$, $\delta_2 = 2{\cdot}155 \cdot 10^{-4}$, $\delta_3 = 1{\cdot}086 \cdot 10^{-6}$.

The stationary profile of the anode was attained with an error less than 1% in all points at a time: A – 334 s, B – 360 s, C – 324 s. The calculated current densities on the surface of the electrodes are given in Tables II and III. For cases A and B, the current distribution and the shape of the anode are symmetrical about the peak. In case C, the increasing temperature of the electrolyte is manifested by an increase of the width of the equilibrium slot and an influence on the current density (Table III). The time dependences of the mean current density, electrolyte temperature at the outlet, and of the pressure loss for this case are given in Table IV.

The equilibrium slot width in the place of the peak was 0·0324, 0·0282, and 0·0485 cm in cases A, B, and C, respectively. The equilibrium slot width in the place most distant from the peak was in case A 0·0633 cm, B 0·0520 cm, and C 0·0945 cm at the electrolyte inlet and 0·1678 cm at the outlet. The course of the machining for the mentioned cases is shown in Figs 4 – 6.

TABLE III

Profile of Anode, Current Distributions on Anode and Cathode and Electrolyte Temperatures in Stationary State for Variant C

x, 10^{-2} m	$\beta(x)$, 10^{-2} m	i_A, 10^4 A/m^2	$-i_K$, 10^4 A/m^2	t, °C
0·000	0·0945	73·3	56·3	20·0
0·093	0·1225	60·7	48·6	23·3
0·178	0·2126	44·4	29·9	25·8
0·255	0·3332	41·7	18·1	27·8
0·326	0·4278	47·7	39·1	30·2
0·389	0·4907	56·2	46·9	33·0
0·447	0·5300	65·1	51·7	35·3
0·500	0·5485	73·3	407·2	41·7[a]
0·553	0·5350	67·9	50·7	48·0
0·611	0·5024	60·2	46·3	50·2
0·674	0·4501	53·1	37·5	52·8
0·745	0·2736	47·9	16·3	55·0
0·822	0·2785	49·5	25·8	56·9
0·907	0·1974	61·7	38·9	59·3
1·000	0·1678	73·2	45·1	62·3

The results show that the equilibrium slot is at the sloped wall of the projection larger than in the place where the parallel walls of the electrodes approach each other. In case *C*, the equilibrium slot width becomes larger with increasing temperature along the line of flow. Polarization of the electrodes makes the current distribution more equal which is undesirable. As a result, the anode–cathode distance in the place of the peak of the projection becomes smaller.

Remarks to Simulation Program

The method of calculation of changes of the anode shape is relatively rapid, the computer time for the calculation of a variant for a given time τ being 10—30 s on an ICL-4-72 type computer, 195 points in the grid, cases *A* and *B*. For case *C*, the calculation of a variant lasted for 5—90 s, 10 s on the average. A 15 × 13 grid was used in all cases.

The program enables to propose the form of the cathode (tool) necessary to achieve the desired shape of the anode (workpiece) in two dimensions. It has to be stressed that a measurement of polarization curves in the region of the working current densities for both electrodes including the anodic current yield is necessary. Approximate calculations neglecting the polarization have only an informative character.

Appendix — Derivation of Eq. (*1*)

The following equation holds in all points of the interelectrode space:

$$div\ i = 0\ . \qquad (A1)$$

The local current density is defined as

$$i = -\varrho_M^{-1}\ \mathrm{grad}\ \varphi\ . \qquad (A2)$$

We assume that the specific resistance ϱ_M of the bubble-electrolyte mixture is a function only of the coordinate x. By substituting Eq. (*A2*) into (*A1*) and after rearrangement we arrive at the Laplace's equation (*1*).

TABLE IV

Dependence of Mean Current Density i, Electrolyte Temperature at Outlet, and Pressure Loss $P_0 - P$ in the Electrolyser on the Duration of Machining

τ, s	i, 10^4 A/m^2	t, °C	$P_0 - P$, kPa
0	29·9	39·6	4·0
20	33·0	41·7	4·4
60	41·1	46·5	6·0
120	51·6	52·0	6·9
180	60·1	56·1	7·1
∞	73·3	62·3	7·7

LIST OF SYMBOLS

a, b	constants of the Tafel equation, V
A	cross-sectional area of flow, m^2
C_i	constants
C_{pE}	specific heat capacity of electrolyte, J/kg K
d_e	equivalent diameter, m
E	potential, V
F	Faraday's constant, 96487 C/mol
F_i	functions, $i = 1-3$, Eqs (*5*)–(*7*)
f, G	functions, Eqs (*45*) and (*8*)
h_i	distance between grid points in the x direction
i	current density, A/m^2
I	total current, A
k_A, k_K	constants, Eqs (*24*) and (*25*)
k_j	distance between grid points in the y direction
k_T	heat transfer coefficient, W/m^2 K
M_A	molar mass of the anode metal, kg/mol
n	number of electrons exchanged in anodic dissolution
n_G	number of electrons exchanged in gas evolution
Δn	shift rate of the anode surface in normal direction, m/s
Nu	Nusselt's criterion
P	absolute pressure of electrolyte, Pa
p_G	current yield in the gas evolution
p_I	current yield in the anode dissolution
Pr	Prandtl's criterion
R	universal gas constant, J/mol K
r	relaxation factor
Re	Reynolds' criterion
Re_M	corrected value of Re, Eq. (*44*)
S_A, S_E	density of the anode metal and of the electrolyte, kg/m^3
T	absolute temperature of the electrolyte, K
T_A, T_K	absolute temperatures of the anode or cathode surface, K
U	terminal voltage of the electrolyser, V
v_y	shift rate of the anode against the cathode, m/s
$\dot{V}_E, \dot{V}_G$	volume rates of flow of electrolyte and gaseous phase, m^3/s
w	channel width, m
x, y	space coordinates, m
α, β	curves expressing the shape of the cathode and anode
γ	stream line, Eq. (*31*)
δ_i	$i = 1-3$, constants in Eq. (*34*)
ξ, η	coordinates
λ	heat conductivity of the electrolyte, W/m K
μ	dynamic viscosity of the electrolyte, kg/m s
ϱ_E, ϱ_M	specific resistances of the electrolyte and gas emulsion, Ωm
τ	time, s
φ	potential, V
ψ	potential, V

Subscripts or Superscripts

A anode
K cathode
n normal component
N new value in the iterations
O value in the point x = a
r equilibrium value
q, s denotation of iterations
s mean value

REFERENCES

1. Mc Geough J. A.: *Principles of Electrochemical Machining*, p. 218. Chapman and Hall, London 1974.
2. Wilson J. F.: *Practice and Theory of Electrochemical Machining*, p. 136. Wiley-Interscience, New York 1971.
3. De Barr A. E., Oliver D. A.: *Electrochemical Machining*, p. 158. Mc Donald, London 1968.
4. Ref. 1, p. 227.
5. Robinson R. A., Stokes R. H.: *Electrolyte Solutions* (in Russian), p. 64. Izd. Inostr. Lit., Moscow 1973.
6. Zuber M.: Chem. Eng. Sci. *19*, 897 (1964).

Translated by K. Micka.